The Tensile Properties of Strain-Crystallizing Vulcanizates. III. The Superiority of Conventional over Peroxide Vulcanizates in Terms of Network Microstructure

M. Van Der Horst, W. J. McGill, C. D. Woolard

Physical and Polymer Chemistry Research Group, Nelson Mandela Metropolitan University, Port Elisabeth, South Africa

Received 29 March 2005; accepted 15 December 2005
DOI 10.1002/app.23902
Published online in Wiley InterScience (www.interscience.wiley.com).

ABSTRACT: It is proposed that, when vulcanization is performed using peroxides, crosslinking leads to a simple network, whereas in conventional vulcanization crosslinking a partially interpenetrating polymer network (PIPN) is formed. Two unfilled polyisoprene networks of similar crosslink density, produced with dicumyl peroxide and 2-bisbenzothiazole-2,2′-disulfide/sulfur formulations, were compared with respect to the effect of strain rate on their stress–strain and hysteresis curves at room and elevated temperatures. At high elongations, the stress–strain curves for peroxide vulcanizates show a steeper upturn than for conventional vulcanizates, but have lower tensile strength and elongation at break. On increasing the extension rate, stress–strain curves for peroxide vulcanizates rise less steeply, while conventional vulcanizates rise more steeply. For both vulcanizates the hysteresis ratio decreases on increasing the rate at which samples are extended and retracted. The effect on conventional vulcanizates is less than on peroxide vulcanizates. It is suggested that chains in peroxide networks disengage increasingly rapidly at higher strains, allowing increased strain-induced crystallization. Rapid strain-induced crystallization leads to low ultimate tensile strength (UTS). In more complex PIPNs, the disengagement and alignment of chains are retarded. The increased nonuniform extension of chains promotes early strain-induced crystallization at low extensions, but overall it reduces the rate of crystallization, which occurs over a wider range of strains. This improves UTS and elongation.
 J Appl Polym Sci 102: 876–884, 2006

Key words: conventional vulcanizate; peroxide vulcanizate; network microstructure; tensile strength; hysteresis; strain-induced crystallization

INTRODUCTION

It is well known that the physical properties of vulcanizates, prepared with different formulations, differ. In general, the properties (other than thermal stability) of conventional vulcanizates, which have mainly polysulfidic crosslinks, are better than those of efficient vulcanizates, with mainly monosulfidic crosslinks, while the properties of peroxide vulcanizates, with carbon–carbon crosslinks, are the poorest.[1,2] Radiation-cured systems, which also contain carbon–carbon crosslinks, display even poorer tensile properties.

Bond energies decrease in the order C—C > C—S > S—S[3] It has been proposed that weak crosslinks are essential for good tensile properties because the low bond energies of polysulfidic crosslinks would allow them to break under stress and reform later.[4,5] Such crosslinks would break under stress before the rubber backbone breaks, resulting in localized relaxation of stress and preventing failure of the network. It has, however, been shown that if broken crosslinks are prevented from reforming, tensile strength is not reduced.[6] Tobolsky and Lyons[7] suggested that the weakness of polysulfidic crosslinks did not play a role at room temperature, but only at vulcanization temperatures, where the mobility of polysulfidic crosslinks allow an internally relaxed network to form. Peroxide vulcanizates, with carbon–carbon crosslinks, are unable to form such relaxed networks. The introduction of polysulfidic crosslinks into a peroxide-cured natural rubber did not increase the tensile strength or flex life of the vulcanizate, and this was attributed to carbon–carbon crosslinks having locked the network in its prestressed state.[3] Lal[3] found that, if polysulfidic crosslinks were converted to mono- and disulfides, there was no appreciable decrease in tensile strength, which led to the conclusion that polysulfidic crosslinks, by themselves, are not responsible for good physical properties, but that other factors following from the curing system, are responsible. Nasir and Teh,[8] however, showed a decrease in ultimate tensile strength (UTS) on converting polysulfidic to monosul-

Correspondence to: C. D. Woolard (Christopher.Woolard@nmmu.ac.za).

Contract grant sponsor: South African National Research Foundation; contract grant number: GUN 2046777.

fidic crosslinks. Gehman[9] suggested that the distribution of crosslinks along the main chain is important in determining properties. Peroxide and radiation curing lead to short chain segments between crosslinks, while the autocatalytic nature of efficient and conventional systems lead to longer chain segments. Grobler and McGill[2] proposed that a heterogeneous distribution of crosslinks within the network was needed for good physical properties. Hamed[10] concluded that vulcanizates of lower crosslink density are more able to blunt crack propagation, and that areas of low crosslink density in a heterogeneous network are able to decrease crack growth, thus increasing physical properties. Others[11] have considered polysulfidic crosslinks to be short chains that form part of the network and which combined with long chains to form a bimodal network. Bimodal networks undergo nonaffine deformation, with the short chains deforming to a lesser degree than the more easily deformable long chains, redistributing strain. In the first paper of the series[12] it was suggested that stiffer chains, ensuing from chain shortening by strain-induced crystalline crosslinks, result in the preferred extension of other, less stiff chains. This alters the network deformation pattern, delays chains being drawn taut to the point of fracture, and leads to higher ultimate tensile stress (UTS) and strain values.

This article proposes different network microstructures for conventional and peroxide-cured vulcanizates, based on differences in the crosslinking mechanism, presents data on the effect of rate and temperature of extension on stress–strain and hysteresis curves for these vulcanizates, and interprets the differences in behavior in terms of the proposed network microstructures.

EXPERIMENTAL

Vulcanizates

Peroxide vulcanizates were prepared by curing *cis*-1,4-polyisoprene (IR) (Nipol IR 2200, Dunlop, Durban, South Africa) with 1 phr dicumyl peroxide (DCP) (Fluka, Steinheim, Germany) to yield a vulcanizate with a crosslink density of 4.66×10^{-5} mol/mL. This compound is referred to as IR/DCP. To obtain a conventional vulcanizate, IR was cured with 3 phr 2-bisbenzothiazole-2,2′-disulfide (MBTS) (Orchem, Sasolburg, South Africa) and 6 phr sulfur (S_8) (AECI, Modderfontein, South Africa) to yield a vulcanizate with a crosslink density of 4.54×10^{-5} mol/mL. This compound is referred to as IR/MBTS and had a polysulfidic crosslink (—S_x—, $x \geq 3$) content of 90.2%. IR/DCP also contained 0.5 phr of the antioxidant *N*-isopropyl-*N*′-phenyl-*p*-phenylenediamine (IPPD) (Bayer, Leverkusen, Germany) and IR/MBTS 1 phr IPPD to prevent oxidation at elevated temperatures. The compounding, vulcanization, and crosslink density determination procedures have been detailed in the first paper of the series.[12]

Determination of polysulfidic crosslink content

A chemical probe was used to determine the percentage polysulfidic crosslinks (—S_x—, $x \geq 3$) present in conventionally cured rubber vulcanizates. The initial crosslink density of the samples were first determined. They were then swollen in *n*-pentane (Saarchem, Midrand, South Africa) for 24 h before they were placed in 5 mL of probe solution, and left under a nitrogen atmosphere in the dark for 2 h. The probe solution consisted of 0.4*M* redistilled 2-propanethiol (Aldrich, Steinheim, Germany) and 0.4*M* piperidine (Saarchem) in *n*-pentane.[13] The samples were then washed with two 10-mL washings of petroleum ether for 1 h each. The samples were dried in a fume hood for 24 h and for another 24 h under high vacuum. The final crosslink density of the samples was then determined. The difference between the initial crosslink density and the final one was due to the loss of polysulfidic crosslinks broken by the probe. The average polysulfidic content of three samples per compound was determined.

Stress–strain measurements

Tensile tests were conducted using an Instron 4411 Tensiometer fitted with a 1-kN load cell, and except where otherwise specified, extensions were done at a crosshead extension speed of 500 mm/min. Extension was either measured by an Instron long travel elastomeric extensometer and expressed as a strain measurement or was measured as the distance (in millimeter) traveled by the upper grip. Extensions at elevated temperatures were conducted in a thermostatted water tank, as described in Paper I of this series.[12] Three different types of sample were used: (1) D size ASTM D 412 dumbbell, (2) custom dumbbell with a gauge length of 8 mm and neck width of 2 mm, and (3) ring-shaped samples (inner diameter 16 mm, outer diameter 20 mm) cut with a nonrotating ring cutter. ASTM dumbbells were used with the extensometer and the latter two samples in the water tank.

Hysteresis measurements

To calculate hysteresis (W_{hys}), the energy recovered by retraction was subtracted from the energy required for extension (W_i). The areas under the extension and retraction curves yielded the required energy densities (W). Experiments were conducted in the water tank when elevated temperatures were required.

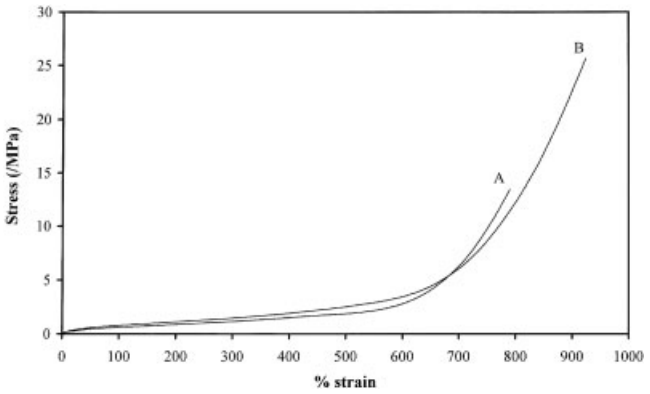

Figure 1 The extensometer, room temperature stress–strain curves of (A) IR/DCP and (B) IR/MBTS.

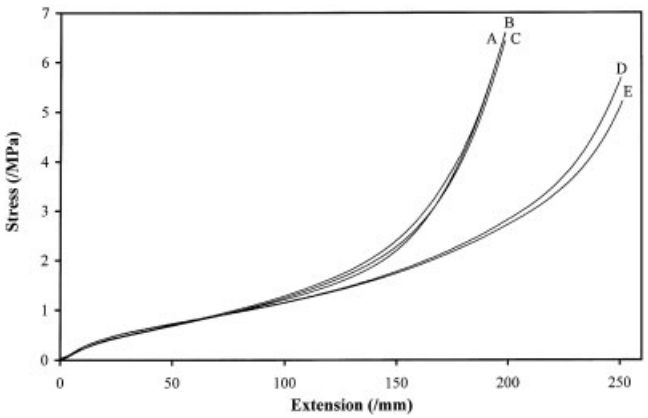

Figure 2 Room temperature and 90°C stress–strain curves of IR/MBTS, extended at different extension speeds (500, 100, and 0.5 mm/min). (A) 500 mm/min, room temperature; (B) 100 mm/min, room temperature; (C) 0.5 mm/min, room temperature; (D) 500 mm/min, 90°C; and (E) 100 mm/min, 90°C.

RESULTS

It is well known that the UTS of peroxide vulcanizates is inferior to that of conventional vulcanizates of similar crosslink density. Figure 1 shows typical room temperature extensometer stress–strain curves for two such vulcanizates. There are two features to note: the IR/DCP curve initially lies below that for the IR/MBTS vulcanizate and, at higher extensions, turns up more rapidly.

Effect of rate and temperature on extension

Strain-induced crystallization, which gives rise to the upturn in the stress–strain curve[12] and to stress relaxation,[14] is time dependent, i.e., nonequilibrium conditions are experienced during the extension of a sample. Ring samples of IR/DCP and IR/MBTS were extended at 500, 100, and 0.5 mm/min at room temperature and at 500 and 100 mm/min at 90°C. Extensions were done to 90% of the UTS values to allow capture of hysteresis data discussed here. Figure 2 shows that there is no significant difference in the room temperature stress–strain curves of IR/MBTS, but at 90°C the curve on fast extension lies slightly above that for the slower extension. With IR/DCP, the reverse applies and the curves on slower extension now show a more rapid upturn. At room temperature, curves on slower extension rise markedly more rapidly, while at 90°C the difference between the curves is much smaller. In Figures 3 and 4 the data is replotted to allow comparison of the curves for the two vulcanizates at room temperature and at 90°C. At room temperature, curves for IR/DCP lie below those for IR/MBTS, but their slopes increase more rapidly at high extensions, stress in IR/MBTS increasing earlier but more gradually. At 90°C the curves are initially similar, but the more rapid increase in slope of IR/DCP is evident at high extensions.

Stress relaxation on slow extension appears more limited and slower (Fig. 5), but this is due to more relaxation having occurred during the extension process. On cessation of extension the stress in IR/MBTS, extended at room temperature to 170 mm, relaxed by 10% when extended at 0.5 mm/min and by 30% when extended at 500 mm/min.

Hysteresis

The effect of extension rate on hysteresis was analyzed on IR/DCP ring samples at extension rates of 500, 100, and 0.5 mm/min at room temperature (Fig. 6) and at 500 and 100 mm/min at 90°C. The first strain cycle of a new sample was measured each time and samples were extended to the same extension. The input energy density (W_i), energy density hysteresis (W_{hys}), and hysteresis ratio (β) are shown in Table I.

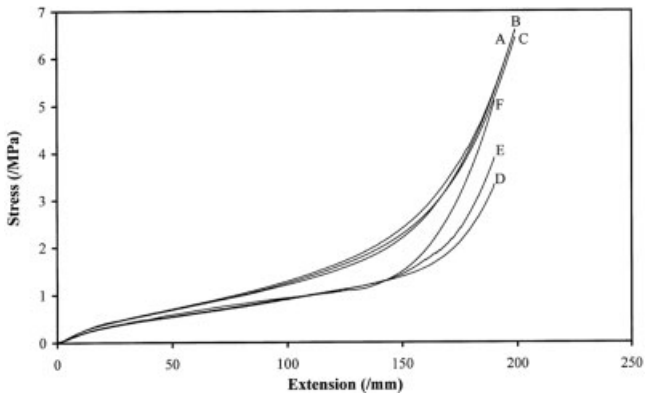

Figure 3 Room temperature stress–strain curves of IR/MBTS and IR/DCP, done at three different extension speeds (500, 100, and 0.5 mm/min). (A) IR/MBTS, 500 mm/min; (B) IR/MBTS, 100 mm/min; (C) IR/MBTS, 0.5 mm/min; (D) IR/DCP, 500 mm/min; (E) IR/DCP, 100 mm/min; and (F) IR/DCP, 0.5 mm/min.

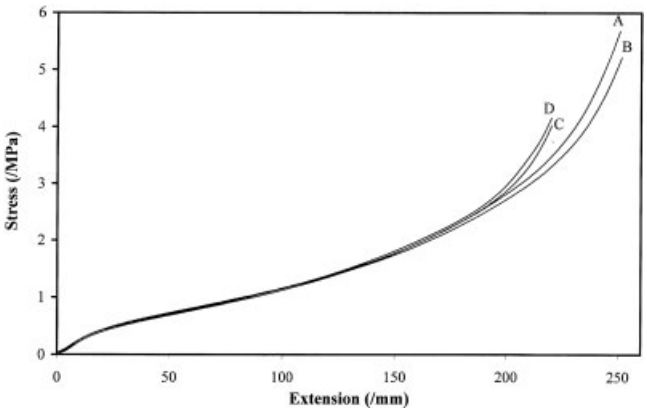

Figure 4 90°C stress–strain curves of IR/MBTS and IR/DCP, done at two different extension speeds (500 and 100 mm/min). (A) IR/MBTS, 500 mm/min; (B) IR/MBTS, 100 mm/min; (C) IR/DCP, 500 mm/min; and (D) IR/DCP, 100 mm/min.

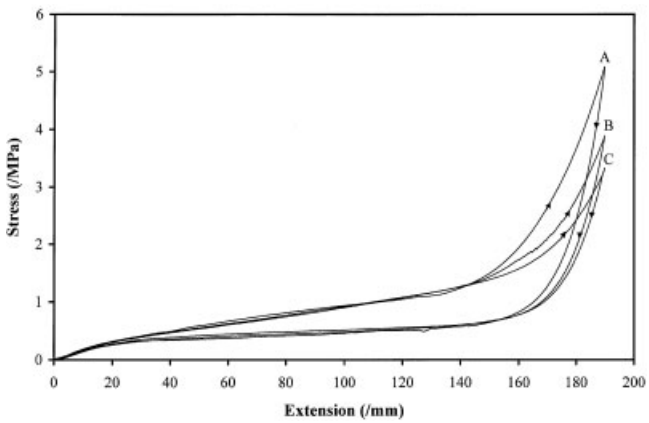

Figure 6 Room temperature strain cycles of IR/DCP done at different extension speeds. (A) 0.5 mm/min; (B) 100 mm/min; and (C) 500 mm/min.

It can be seen in Figure 3 that in IR/DCP the room temperature stress on slow extension rose more rapidly than on fast extension, and on cyclic loading the stress–strain curves on retraction likewise lie above those for slower extension (Fig. 6). When the slope of the extension curve rises more rapidly, as on slower extension, the slope of the initial portion of the return curve is also steeper. At 90°C strain curves at different rates of extension were very similar, though the curve for slow extension did lie marginally above that for fast extension. Room temperature strain cycles for IR/MBTS were very similar, but at 90°C the faster strain cycle lay marginally above that for slower extension. The data are given in Table I.

DISCUSSION

Vulcanization reactions and network microstructure

It is proposed that differences in the tensile properties of IR/MBTS and IR/DCP vulcanizates can be ascribed to differences in the network microstructure that result from differences in the reaction mechanism that leads to crosslinks.

Crosslinking of polyisoprene by peroxides involves peroxide decomposition and the formation of a radical on the polymer chain by hydrogen abstraction.[15,16] The reaction sequence for crosslinking of natural rubber and model compound 2,6-dimethyl-octa-2,6-diene has been established as involving reaction between polymer radicals on neighboring chains, and for reaction with DCP, has a crosslinking efficiency of unity.[15,16] In accelerated sulfur vulcanization interaction of sulfur with accelerators leads to the formation of accelerator polysulfides[17–19] which, in the absence of zinc compounds, constitute the active sulfurating agent.[13,17–22] Many reviews and articles[13,17,23] suggest that accelerator-terminated polysulfidic pendent groups, the precursors to crosslink formation, can crosslink by disproportionation or by reaction with the polymer chain, or that both mechanisms may ap-

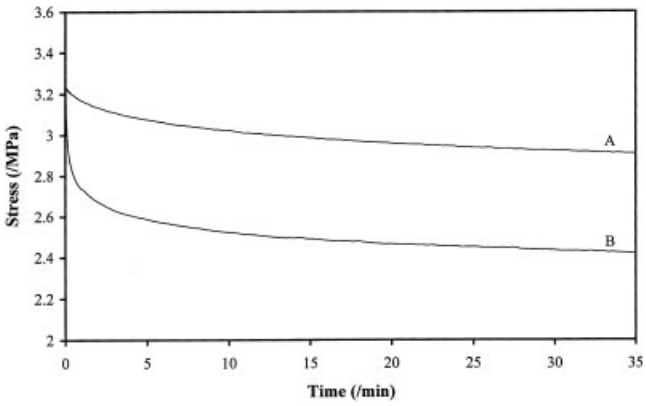

Figure 5 Stress relaxation of IR/MBTS following slow (A) 0.5 mm/min and fast (B) 500 mm/min extension.

TABLE I
The Energy Density Hysteresis Values of IR/MBTS and IR/DCP at Different Temperatures and Extension Speeds

Temperature (°C)	Extension speed (mm/min)	W_i (kJ/m^2)	W_{hys} (kJ/m^2)	β
IR/MBTS				
	500	0.354	0.161	0.456
	100	0.340	0.158	0.467
23	0.5	0.338	0.159	0.471
	500	0.455	0.064	0.141
90	100	0.437	0.068	0.156
IR/DCP				
	500	0.189	0.069	0.369
	100	0.201	0.077	0.382
23	0.5	0.224	0.094	0.419
	500	0.316	0.029	0.094
90	100	0.326	0.037	0.113

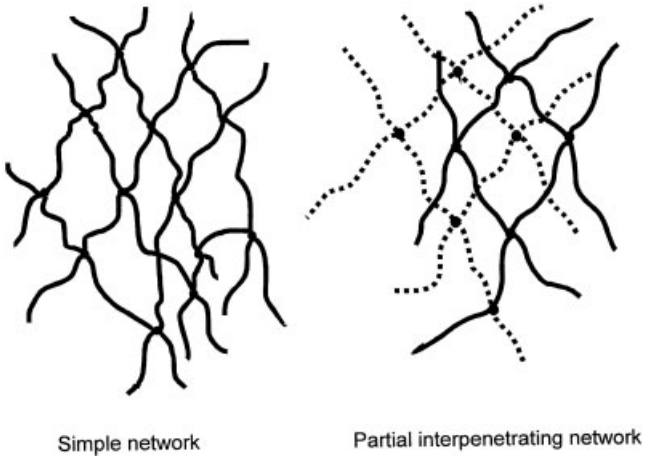

Figure 7 An idealized, schematic representation of the unraveled network microstructures of a simple and partial interpenetrating networks.

ply. More recent studies have shown that disproportionation occurs slowly in the absence of zinc compounds, while pendent group-chain reactions are limited.[21] Instead, crosslinking results from reaction between accelerator terminated polysulfidic pendent groups and polysulfidic thiols.[24–27] Polysulfidic thio pendent groups may form via exchange reactions[19,24,28] between polysulfidic pendent groups and thio acids liberated on pendent group formation, while on reaction with sulfur the thio acids themselves can act as accelerators.[19,25,27] In MBTS systems, the thio-acid is MBT, a known accelerator.[26]

Since crosslinking with a peroxide involves reaction between chain radicals, this necessitates reaction between immediately adjacent chains. It is suggested that on swelling the network will expand as depicted schematically in Figure 7 for a two-dimensional network. Chains in the randomly coiled network will undergo a similar disengagement or unraveling when extended under load, the unraveled chains becoming partially aligned. This will be referred to as a simple network.

In accelerated sulfur vulcanization the length of polysulfidic pendent groups and polysulfidic thiols will depend on the number of sulfur atoms present, and as a consequence of their length, these groups will protrude some distance into the adjacent polymer mass. Crosslinking, resulting from reaction between such groups, is less likely to involve groups on immediately adjacent chains, and crosslinking will occur between nonadjacent chains. It is suggested that this leads to a partially interpenetrating network (PIPN) which, on swelling or extension under load, will unravel and devolve as depicted in Figure 7. Interpenetration may occur locally between networks A and B. Chains that locally form part of network A, interpenetrated by network B (and possibly C, D, etc.), may, in a neighboring locality, be linked to network B, which is now interpenetrated by chains constituting other networks. The net result is not an ideal interpenetration of networks A and B, as most frequently referred to in the literature,[11,29] but one in which the degree and nature of interpenetration varies locally. As discussed later, it is proposed that differences in the properties of peroxide and conventional vulcanizates can be ascribed to differences in the strain-induced crystallization of simple and PIPNs.

Microstructure and strain-induced crystallization

In a previous paper[12] it was proposed that the upturn in the stress–strain curve and the resulting high UTS of vulcanizates that undergo strain-induced crystallization are due to chain shortening resulting from the formation of strain-induced crystalline crosslinks in the network. Shorter chains have lower entropies, are stiffer, and require a larger force for their extension. Stiffening a chain delays it from being drawn taut to the point of failure, whereas other, less stiff chains preferentially deform. This alters the network deformation pattern and delays rupture to higher elongations and UTS values. To examine differences in the tensile properties of conventional and peroxide vulcanizates, it is necessary to look more closely at the deformation of the proposed networks and the development of strain-induced crystal nuclei.

In a network conformational changes resulting from rotation about carbon–carbon bonds will allow extension of the network under load. No chain can extend in isolation, and conformational changes in a given chain require the cooperative movement of segments on neighboring chains. The slow response or temporary entrapment of sequences of an extending chain, or its attached chains, will impede its movement, and may lead to the transient localized over extension of a freed segment of the chain. This will markedly affect the entropy of the over-extended segment. Any localized reorientation of a chain segment will require that adjacent chains, at least partially, comply with this conformation. There are various models which suggest that some degree of localized order exists within amorphous polymers,[30] and locally, the overall decrease in the entropy of the chain and its neighbors in the region may be sufficient to initiate nucleation.

Microstructure and UTS

In a simple network there will be some intertwining or entanglement of the initially randomly coiled chains, but these will disengage or be released gradually as chains extend and the network unravels. As the degree of alignment increases, further alignment will become progressively easier. Hence the rate of strain-

induced crystallization accelerates and the stress–strain curve rises more rapidly at high strains (Fig. 1).

In a PIPN the intertwining and entanglement of chains will be more complex and its extension and the release or unraveling of chains of one local network from the chains in the second, superimposed network, will be slower. The stress–strain curve for IR/MBTS lies above that for IR/DCP right from the outset, i.e., well before strain-induced crystallization occurs and influences the upturn in the stress–strain curve. This is attributed to the more viscous PIPN in which chain deformation is impeded or slowed by extensive interpenetration, intertwining, and entanglement of chains in different networks.

Extension of chains will occur less uniformly than in a simple network and may lead to localized entropy conditions favorable for the development of strain-induced nuclei at lower extensions, contributing to the higher slope at low strains. Overall, the PIPN will have a retarding effect on nucleation and, in particular, on the ease of chain alignment at high strains. Thus at higher strains the rate of strain-induced crystallization will increase less rapidly than with simple networks. This is reflected by the slower rate of crystallization and more gradual upturn in the stress–strain curve (Fig. 1). Thus, while nucleation in a PIPN is promoted at low extensions, overall rates of nucleation are reduced, and fewer nuclei form. Such slower rates of nucleation in sulfur-cured NR vulcanizates when compared with those in peroxide-cured vulcanizates have been observed.[31]

Microstructure and elongation

Rapid crystallization and the accompanying chain shortening in simple networks lead to a network in which chains or chain sequences are drawn taut to the point of rupture at fairly low elongations. Where PIPNs crystallize, however, chain shortening is more gradual and, at any elongation, there are more extensive zones in which long chains persist and hence can extend, and thus larger extensions are reached before network failure. Hydrostatic weighing experiments showed that at any elongation the extent of crystallinity developed at equilibrium (after stress relaxation) in IR/DCP and IR/MBTS was similar at similar elongations. It is the slower crystallization of IR/MBTS during the extension process, as shown by the slower upturn in the stress–strain curves (Fig. 1), that allows the network to extend further before failing. The slow crystallization is analogous to delayed crystallization at elevated temperatures discussed in an earlier paper.[12] Samples extend to larger elongations before failing.

Effect of temperature and crosslink density

In an earlier paper,[12] it was shown that at room temperature IR/MBTS has tensile properties (UTS and elongation) superior to IR/DCP over a range of crosslink densities. At lower crosslink densities the UTS and elongation at break of both vulcanizates increased at elevated temperatures, IR/MBTS vulcanizates retaining their superiority relative to IR/DCP. The difference can be attributed to slower strain-induced crystallization in IR/MBTS at both room and elevated temperatures. However, at higher crosslink densities the high temperature UTS and elongation at break of all vulcanizates are dramatically lower than at room temperature.[12] Chain shortening is needed to divert extension to other chains in the network and to prevent chains from being drawn taut and leading to premature failure. At elevated temperatures larger elongations are required for the entropy to decrease sufficiently for nucleation to occur, and at higher crosslink densities, taut chains develop in the now more slowly crystallizing vulcanizates before strain-induced crystallization and the redistribution of the chain deformation pattern can occur. This explains why the UTS and elongation at break of both vulcanizates are dramatically lower at elevated temperatures. Furthermore, the UTS and elongation at break in IR/MBTS now drop below those for IR/DCP[12]; rates of nucleation are reduced both by an increase in temperature and by slow crystallization in the more complex PIPN.

Effect of temperature and rate of extension

The rate of extension at room temperature has little effect on the stress–strain curve for IR/MBTS (Fig. 3), suggesting that the rate of disentanglement of chain segments controls nucleation. Nevertheless, Table I shows a small decrease in W_i with a decrease in rate of extension. Slower extension facilitates the disentanglement of chains, allowing their more uniform extension and reduces the extent of strain-induced crystallization, which would increase the slope of the stress–strain curve. With IR/DCP, the upturn increases more steeply on slow extension and is attributed to the formation of more strain-induced crystalline crosslinks, the rate of formation of which is time-dependent. Table I also shows that with slower extension and more time for strain-induced crystallization in IR/DCP, there is an increase in the work (W_i) required to extend vulcanizates to a given extension at both room temperature and 90°C.

High temperatures will facilitate disentanglement and reduce the resistance to deformation (or viscosity) of the IR/MBTS PIPN, and the early section of the high and low temperature stress–strain curves coincide (Fig. 2), the increased entropic retractive forces at elevated temperatures being countered by enhanced

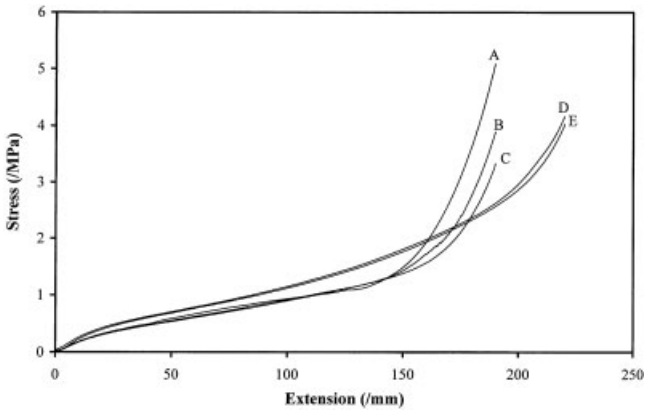

Figure 8 The room temperature and 90°C stress–strain curves of IR/DCP, extended at different extension speeds (500, 100, and 0.5 mm/min). (A) 0.5 mm/min, room temperature; (B) 100 mm/min, room temperature; (C) 500 mm/min, room temperature; (D) 100 mm/min, 90°C; and (E) 500 mm/min, 90°C.

disentanglement (lower viscosity). Easier disentanglement will reduce the rate of nucleation at low extensions and, coupled with the overall reduced rate of nucleation at elevated temperatures, will ensure that the stress–strain curves drop below those at room temperature (Fig. 2). In the early stages of extension, before the formation of strain-induced crystallites, the high temperature stress–strain curves for the IR/DCP lie above those at room temperature (Fig. 8). This is to be expected in terms of higher entropy at elevated temperatures. However, larger extensions (a larger decrease in entropy) are required before strain-induced crystallization can occur; the upturn in the high temperature stress–strain curves is delayed, and the curves rise less steeply due to the slower rate of nucleation (Fig. 8). The reduced rate of nucleation at the elevated temperatures minimizes the difference between the curves for rapid and slow extensions.

High temperatures will facilitate chain disentanglement, and the high temperature stress–strain curves for IR/DCP and IR/MBTS coincide over a large extension range (Fig. 4). However, faster nucleation, resulting from the easier alignment of chains in IR/DCP at high extension, ensures that the stress–strain curves rise above those for IR/MBTS at high strains. In a PIPN chain alignment at high strains does not occur as readily, while slow extension allows for more disentanglement of chain segments, decreasing the rate of nucleation even further. Thus, while in IR/DCP networks slow extension allows for slightly more crystalline crosslinks to form, stiffening chains and increasing the rate at which the stress increases, the slope of stress–strain curves for IR/MBTS rise more slowly on slow extension.

The effect of slower nucleation at elevated temperatures is also demonstrated by the extent of stress relaxation observed on cessation of extension. The rate of strain-induced crystallization increases with strain, and at room temperature this leads to a decrease in the extent of postextension relaxation in both vulcanizates, while at elevated temperatures slow crystallization results in the extent of postextension relaxation increasing with strain.[14] The degree of postextension relaxation in IR/MBTS is much larger than in IR/DCP,[14] and this further highlights the differences in the rate of strain-induced crystallization of the two networks, chain disentanglement in simple networks occurring very readily at elevated temperatures, resulting in less postextension crystallization.

Hysteresis

Increased strain-induced crystallization on slower extension of IR/DCP leads to higher hysteresis, as seen in Table I, where β, the ratio of energy density of hysteresis (W_{hys}) to the energy input density (W_i), increases. With IR/MBTS, too, β increases with a decrease in rate of extension, but the reduced rate of strain-induced crystallization on slow extension results in rates of extension having a much smaller effect on β, which at room temperature changes by 3% for extension rates of 500 and 0.5 mm/min, compared with a 13% change for IR/DCP vulcanizates. At higher temperatures the strain cycles done at different extension rates are very similar, but the slight increase in β with a decrease in extension rate for both vulcanizates (Table I) shows that more crystallization does occur between the extension and retraction cycles. At 90°C, too, the effect of rate of extension on β is smaller for IR/MBTS, viz. 10 and 20% for extension rates of 500 and 100 mm/min respectively. The data in Table I emphasize differences in the behavior of IR/MBTS and IR/DCP networks and support the contention in an earlier paper[14] that hysteresis in strain-crystallizing vulcanizates results largely from differences in the extent of strain-induced crystallization of extension and retraction.

Variable sample crystallization

The effect of rate of extension on hysteresis was further examined by varying the amounts of strain-induced crystallization that occurs in different parts of dumbbell samples. The degree of extension, and hence strain-induced crystallization, that develops in the neck and broader base of dumbbells will differ, the extension of the tensometer head giving a composite measure of extension of the neck, shoulders, and base of the dumbbell. By varying the width of the base the extension ratio of the neck to the base can be changed.

At low strains no strain-induced crystals develop in the test piece and the return curves for the standard and narrow based dumbbells coincide. At higher

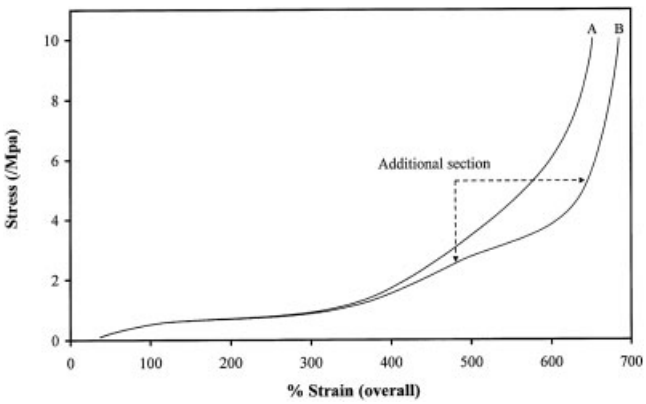

Figure 9 The return parts of the strain cycles of standard "D" size (A) and narrow base dumbbells (B) strained to 10 MPa.

strains strain-induced crystals develop in the neck and raise the stress required for its continued deformation. Thus, extension of the neck is slowed down at the expense of more deformation of the base, extension in this area now becoming noticeably greater in narrow based than in standard dumbbells. The initial portion of the return curves no longer coincide, the narrow based dumbbell having extended further because of the more ready extension of its base. At still higher extensions strain-induced crystallization will occur in the base of both dumbbells. The extension curves remain uniform, while the return curves for the narrow based dumbbell includes a section in which the curve decreases less steeply (Fig. 9). At the commencement of the return curve further rapid crystallization, accompanied by stress relaxation, will occur.[31–37]

The base will have suffered a lower strain than the neck, and since the lower the strain, the higher the postextension relaxation,[14] a large proportion of this rapid crystallization will occur in the base. Thus, at the commencement of the return cycle considerable strain-induced crystallization also occurs in the base area of the narrow based dumbbell, and the return stress–strain curve drops more rapidly than for the standard dumbbell. The retraction curve for the narrow based dumbbell now comprises of what is essentially a superimposition of two retraction curves, one for the neck and one for the base. Since the base has suffered less extension, chains surrounding the crystallites will have higher entropies than do chains in the neck region. This means that, on melting, chains from crystallites enter regions of higher entropy, and melting in this region is likely to occur in preference to the melting of crystallites in the neck. The load borne by the neck and base is obviously the same, but the stress in the base is less. At any extension the base will be at a smaller strain than the neck, and in terms of the stress–strain curve, a small change in stress in the base will be accompanied by a big change in strain, accounting for the large decrease in the strain when compared with the rate at which the stress decreases in Figure 9. Melting of crystals will not be confined to the base, but melting in this region will dominate. Once crystals in the base have melted, the retraction curve conforms to that of the standard dumbbell. There will of course be a similar differential in the melting of crystals in the neck and base of the standard dumbbell, but the difference will not be as marked, and the retraction curve does not show as great a leveling off effect as is evident for the narrow based dumbbell in Figure 9.

CONCLUSIONS

Reactions that result in crosslink formation in peroxide and conventional vulcanizates will lead to differences in network microstructure. With peroxides crosslinking between chain radicals will result in a simple network, and in conventional vulcanizates crosslinking between polysulfidic pendent groups and polysulfidic thiols will result in a partially interpenetrating polymer network. Differences in tensile properties and hysteresis of these vulcanizates are attributed to differences in the ease and rate at which chains in these networks disentangle on straining. The networks respond differently to the rate of loading, the rate of strain-induced crystallization controlling the response of simple networks, and the rate of disentanglement, the response of PIPNs. The slower, delayed crystallization in conventional vulcanizates accounts for their superior tensile strength and higher hysteresis. Rate of strain has a lesser effect at elevated temperatures where rates of crystallization are slower.

References

1. Greensmith, H. W.; Mullins, L.; Thomas, A. G. In The Chemistry and Physics of Rubber-like Substances; Bateman, L., Ed.; Maclaren and Sons, Ltd: London, 1963; Chapter 10.
2. Grobler, J. H. A.; McGill, W. J. J Polym Sci Part B Polym Phys 1994, 32, 287.
3. Lal, J. Rubber Chem Technol 1970, 43, 664.
4. Bateman, L.; Cunneen, J. J.; Moore, C. G.; Mullins, L.; Thomas, A. G. In The Chemistry and Physics of Rubber-like Substances; Bateman, L., Ed.; Maclaren and Sons, Ltd: London, 1963; p 715.
5. Cox, W. L.; Parks, C. R. Rubber Chem Technol 1966, 39, 785.
6. Brown, P.; Porter, M.; Thomas, A. G. Presented at the International Rubber Conference (Rubbercon '87), Harrogate, UK, June 1987.
7. Tobolsky, A. V.; Lyons, P. F. J Polym Sci Part A-2: Polym Phys 1968, 6, 1561.
8. Nasir, M.; Teh, G. K. Eur Polym Mater 1988, 24, 733.
9. Gehman, S. D. Rubber Chem Technol 1969, 42, 659.
10. Hamed, G. R. Rubber Chem Technol 1983, 56, 244.
11. Erman, B.; Mark. J. E. Structures and Properties of Rubberlike Networks; Oxford University Press: New York, 1997; Chapter 13.
12. Van der Horst, M.; McGill, W. J.; Woolard, C. D. J Appl Polym Sci 2006, 101, 1562.

13. Saville, B.; Watson, A. A. Rubber Chem Technol 1967, 40, 100.
14. Van der Horst, M.; McGill, W. J.; Woolard, C. D. J Appl Polym Sci 2006, 101, 2423.
15. Loan, L. D. Rubber Chem Technol 1967, 40, 149.
16. Moore, C. G.; Watson, W. F. J Polym Sci 1956, 19, 237.
17. Nieuwenhuizen, P. J; Reedijk, J; van Duin, M.; McGill, W. J. Rubber Chem Technol 1997, 70, 368.
18. Coleman, M. M.; Shelton, J. R.; Koenig, J. L. Rubber Chem Technol 1973, 46, 957.
19. Gradwell, M. H. S.; Morgan, B.; McGill, W. J. J Appl Polym Sci 1995, 56, 1581.
20. Shelton, J. R.; McDonel, E. T. Rubber Chem Technol 1960, 33, 342.
21. Geyser, M.; McGill, W. J. J Appl Polym Sci 1999, 60, 431.
22. Versloot P.; Haasnoot, J. G.; Reedijk, J.; van Duin, M.; Duynstee, E. F. J.; Put, J. Rubber Chem Technol 1994, 67, 252.
23. Porter, M. In The Chemistry of Sulfides; Tobolsky, A. V., Ed.; Wiley: New York, 1968; p 165.
24. Morgan, B.; McGill, W. J. J Appl Polym Sci 2000, 76, 1395.
25. Shelver, S. R.; Shumane, M.; Gradwell, M. H. S.; McGill, W. J. J Appl Polym Sci 1999, 74, 1371.
26. Van der Horst, M.; Hendrikse, K. G.; Woolard, C. D. J Appl Polym Sci 2003, 89, 47.
27. Nieuwenhuizen, P. J; Ehlers, A. W.; Haasnoot, J. G.; Janse, S. R.; Reedijk, J.; Baerendse, E. J. J Am Chem Soc 1999, 121, 163.
28. Guiliani, B. V. M. K.; McGill, W. J. J Appl Polym Sci 1995, 57, 1391.
29. Sperling, L. H. Introduction to Physical Polymer Science; Wiley-Interscience: New York, 1986; Chapter 2.
30. Sperling, L. H. Introduction to Physical Polymer Science; Wiley-Interscience: New York, 1986, Chapter 5.
31. Toki, S.; Sics, I.; Ran, S.; Liu, L.; Hsiao, B. S.; Murakami, S.; Tosaka, M.; Kohjiya, S.; Poompradub, S.; Ikeda, S.; Tsou, A. H. Rubber Chem Technol 2004, 77, 317.
32. Toki, S.; Fujimaki, T.; Okuyama, M. Polymer 2000, 41, 5423.
33. Murakami, S.; Senoo, K.; Toki, S.; Kohjiya, S. Polymer 2002, 43, 2117.
34. Trabelsi, S.; Albouy, P.A.; Rault, J. Macromolecules 2003, 36, 7624.
35. Trabelsi, S.; Albouy, P.A.; Rault, J. Rubber Chem Technol 2004, 77, 303.
36. Tosaka, M.; Murakami, S.; Poompradub, S.; Kohjiya, S.; Ikeda, Y.; Toki, S.; Sics, I.; Hsiao, B. S. Macromolecules 2004, 37, 3299.
37. Toki, S.; Sics, I.; Hsiao, B. S.; Tosaka, M.; Poompradub, S.; Ikeda, Y.; Kohjiya, S. Macromolecules 2005, 38, 7064.